AIIM

Association for Information and Image Management

1100 Wayne Avenue, Suite 1100
Silver Spring, Maryland 20910

301/587-8202

Centimeter

Inches

MANUFACTURED TO AIIM STANDARDS
BY APPLIED IMAGE, INC.

1 of 1

Conf-940393--1

LA-UR- 94-1057

Title: KINETIC EFFECTS NEAR THE MAGNETOPAUSE

Author(s): S. Peter Gary, NIS-1
Dan Winske, X-1
Michael E. McKean, University of California
Stephen A. Fuselier, Lockheed Palo Alto Research Laboratory
Richard E. Denton, Dartmouth College
Brian J. Anderson, Applied Physics Laboratory

Submitted to: Proceedings for the AGU Chapman Conference on Physics of the Magnetopause
14-18 March 1994
San Diego, CA

MASTER

Los Alamos
NATIONAL LABORATORY

KINETIC EFFECTS NEAR THE MAGNETOPAUSE

S. Peter Gary and Dan Winske
Los Alamos National Laboratory, Los Alamos, NM 87545

Michael E. McKean
University of California, San Diego, La Jolla, CA 92093

Stephen A. Fuselier
Lockheed Palo Alto Research Laboratory, Palo Alto, CA 94304

Richard E. Denton
Dartmouth College, Hanover, NH 03755-3528

Brian J. Anderson
Applied Physics Laboratory, Johns Hopkins University, Laurel, MD 20723

24 March 1994

Abstract

Boundary conditions for magnetopause processes such as reconnection can be understood by studying the properties of magnetosheath plasma as it flows toward this transition. This manuscript reviews the role of electromagnetic ion cyclotron instabilities in constraining ion temperature anisotropies in the magnetosheath. Linear Vlasov theory and hybrid computer simulations have demonstrated that the inverse correlation between the proton anisotropy and the parallel proton β observed from AMPTE/CCE in the subsolar sheath is due to wave-particle scattering by ion cyclotron anisotropy instabilities. Recent research on this topic is reviewed and the application of this inverse correlation to a successful bounded anisotropy model of proton temperatures in the sheath is described.

This manuscript describes a recent development in the theory of microscopic, i.e. kinetic, physics upstream of the Earth's magnetopause. Therefore, although the primary thrust here will be the same as that of my invited talk at the Conference, some of the details will be different. In particular magnetosheath observations of magnetic fluctuations near the proton cyclotron frequency are addressed in *Anderson* [1994] and will not be treated in detail here.

The context of my presentation and of this manuscript can be established by quoting several other speakers at this Conference. George Siscoe said that, in order that an issue be regarded as of critical importance to future magnetopause studies, it should meet at least one of several criteria. One of these criteria was that "microphysics sets qualitative macrophysics." The concept that small scale physics determines a condition on plasma parameters characterizing the large scale magnetosheath is indeed central to the research presented here. Harry Petschek noted that, to get drag in fluid dynamics, viscosity is necessary, but that its value is not important in subsonic flow. Similarly, although the plasma physics described here depends in a detailed way on the small-scale processes of fluctuation growth and wave-particle scattering, the result, an upper bound on the proton temperature anisotropy, is independent of microscopic quantities such as wave amplitudes or transport coefficients. Finally, Rick Elphic, speaking about a different problem, said, "This is something we should have done in 1980." Indeed, the theoretical tools for the solution of the problem I will describe have been available since the publication of *Kennel and Petschek* [1966]. What we have done is to use the linear theory formalism and the instability threshold concept of that pioneering paper in a new way which, I believe, can be applied not only to magnetospheric and magnetosheath plasmas, but to any space plasma in which microinstabilities are driven to sufficiently large amplitude.

It is well established that heating at the bow shock and magnetic field line draping against the magnetopause imply the development of a proton temperature anisotropy $T_{\perp p}/T_{\parallel p} > 1$, where $\perp$ and $\parallel$ refer, respectively, to directions perpendicular and parallel to the background magnetic field $\mathbf{B}_o$. Such an anisotropy has been observed frequently in the Earth's magnetosheath [*Tsurutani et al.*, 1982; *Sckopke et al.*, 1990; *Anderson et al.*, 1991].

In the terrestrial magnetosheath this nonthermal property leads to the growth of two distinct instabilities and the observation of corresponding enhanced magnetic fluctuations at frequencies below the proton cyclotron frequency Ω_p [*Sckopke et al.*, 1990; *Song et al.*, 1993; *Anderson*, 1994]. Mirror-like magnetic fluctuations arise from the growth of the mirror instability, have frequencies ω_r much less than Ω_p, and are primarily compressive, that is, $\delta\mathbf{B} \parallel \mathbf{B}_o$. In contrast growth of the proton cyclotron anisotropy instability leads to enhanced proton-cyclotron-like fluctuations at $\omega_r \lesssim \Omega_p$ with predominantly transverse fluctuating fields, i.e., $\delta\mathbf{B} \perp \mathbf{B}_o$. The relatively tenuous, hot, anisotropic doubly ionized helium in the sheath can drive the helium cyclotron anisotropy instability; its magnetic fluctuations are observed in the sheath at frequencies below the helium cyclotron frequency [*Anderson et al.*, 1994]. Here I will primarily address the first two modes and refer the reader to *Denton et al.* [1994a] and *Gary et al.* [1994b] for further discussions of the theoretical properties of the helium cyclotron instability.

Anderson and Fuselier [1993] and *Anderson et al.* [1994] used AMPTE/CCE observations to study the subsolar magnetosheath downstream of quasi-perpepndicular bow shocks during times when the magnetosphere was strongly compressed by the solar wind. These observations showed that proton-cyclotron-like fluctuation spectra were predomiant at $\beta_{\parallel p} \lesssim 1$, whereas mirror-like spectra constituted the majority of observations at β values large compared to unity. These authors also showed that the proton temperature anisotropies exhibited a relatively small variation for a given value of $\beta_{\parallel p}$ and that a least-squares fit to the data over the range $0.02 \lesssim \beta_{\parallel p} \lesssim 10.0$ yielded the result

$$\frac{T_{\perp p}}{T_{\parallel p}} - 1 = \frac{0.85}{\beta_{\parallel p}^{0.48}} \tag{1}$$

where $\beta_{\parallel p} \equiv 8\pi n_p T_{\parallel p}/B_o^2$. Similar anisotropy/$\beta$ inverse correlations in the magnetosheath have been observed by *Phan et al.* [1994] and *Fuselier et al.* [1994].

My collaborators and I have interpreted this observation using both linear Vlasov theory and hybrid simulations. I will first discuss linear theory results using the formalism and notation of Chapter 7 of *Gary* [1993].

It has long been known that the thresholds of both the proton cyclotron anisotropy instability and the mirror instability qualitatively satisfy the same type of inverse correlation between proton temperature anisotropy and parallel β that is represented by the observations of Equation (1) [*Gary et al.*, 1976]. To quantify this relationship, we assumed that γ_m, the instability growth rate maximized over all wavevectors, held a constant value of $0.01\Omega_p$ at the thresholds of both growing modes, and used computer evaluations of the unapproximated linear Vlasov dispersion equation to determine the corresponding temperature anisotropies. For each of these instabilities we then plotted these threshold anisotropies as functions of $\beta_{\|p}$ and, in both cases, used a standard least-squares fitting procedure to obtain analytic expressions for the corresponding relationships. Our results for the range $0.01 \leq \beta_{\|p} \leq 10.0$ are for the mirror instability

$$\frac{T_{\perp p}}{T_{\|p}} - 1 = \frac{0.97}{\beta_{\|p}^{0.61}} \tag{2}$$

and for the proton cyclotron anisotropy instability

$$\frac{T_{\perp p}}{T_{\|p}} - 1 = \frac{0.64}{\beta_{\|p}^{0.40}} \tag{3}$$

Although the $\beta_{\|p}$ value of the crossover point of the two threshold curves in Figure 1 can vary with different choices of γ_m and inclusion of the range of He^{++} densities observed in the sheath *Gary et al.* [1993a], it is generally true that the proton cyclotron instability has the lower threshold anisotropy at $\beta_{\|p} \lesssim 1$ and the mirror instability has the lower threshold at β values considerably larger than unity. Thus, if a strong anisotropy were suddenly imposed on a plasma as, for example, at the quasi-perpendicular shock, the system would be unstable to both modes and both types of fluctuations might be observed. On the other hand, if the proton anisotropy were relatively weak so that the plasma was stable to the growth of both modes and that anisotropy were gradually increased, as might happen under the more slowly changing sheath conditions downstream of the shock, Figure 1 suggests that the local β value would determine which instability would first arise. The presumption that that growing mode would also dominate the magnetic fluctuation spectrum leads to the interpretation that proton-cyclotron-like spectra should primarily be observed at low β and mirror-like spectra at high β, in agreement with the observations.

Yet the identification of enhanced fluctuations from a particular instability in either spacecraft data or computer simulations does not necessarily imply that that instability dominates the wave-particle processes which help determine plasma properties. The simulations of *McKean et al.* [1992b, 1994] have shown that, even at relatively high β, the mirror instability may be less effective than the proton cyclotron anisotropy at reducing $T_{\perp p}/T_{\|p}$ under conditions characteristic of the magnetosheath.

This result has been illustrated in a different way by Figure 2 which plots late-time results from a series of initial-value hybrid simulations [*Winske and Omidi*, 1993]. Each run was begun with ion temperature anisotropies large enough to excite rapid instability growth; the individual points in the figure correspond to late-time results reflecting the proton heating and reduction of the temperature anisotropy to the condition of relatively weak instability growth. The solid squares represent the results of one-dimensional simulations at $\mathbf{k}\times\mathbf{B}_o = 0$, a condition permitting only ion cyclotron instabilities to grow. The "X" symbols represent results of one-dimensional simulations allowing only wavevectors strongly oblique to the background magnetic field; in these simulations only the mirror instability was able to increase in amplitude. The open squares illustrate late-time anisotropies from two-dimensional hybrid simulations which permit a broad range of wavevector direction and which therefore have allowed both ion cyclotron and mirror instability to grow. The simulations which involve growth of ion cyclotron instabilities yield late-time results which show the same proton anisotropy/β inverse correlation as the observations, whereas the one-dimensional computations which permit the growth of only the mirror instability do not resemble the observed results. This result supports the hypothesis that ion cyclotron instabilities are the source of the inverse correlation; the picture is that the relatively short wavelengths of these instabilities are very efficient at scattering and reducing the proton temperature anisotropy to the threshold condition, whereas the mirror-like fluctuations are less efficient at producing wave-particle interactions and, when they do interact with the protons, produce changes in the protons that are not readily characterized as a reduction of $T_{\perp p}/T_{\parallel p}$.

Initial value simulations provide insight into the wave-particle interactions associated with ion cyclotron anisotropy instabilities, and provide a useful model for the study of plasma evolution downstream of a quasi-perpendicular shock, where ion temperature anisotropies are suddenly introduced and instabilities lead to a subsequent reduction of those anisotropies. In the plasma depletion layer, by contrast, macroscopic forces lead to a more gradual compression of the magnetic field and to a consequent increase in ion ansotropies. In such a situation, we believe that the model of *Kennel and Petschek* [1966] and *Manheimer and Boris* [1977] is appropriate: a macroscopic driving force which continually pushes the plasma toward increased anisotropy is balanced by the consequences of microscopic effects reducing this anisotropy so that a balanced, relatively steady-state condition is established which corresponds to an instability threshold.

To represent the conditions of this steady-state balance between macroscopic and microscopic effects, we have modified the one-dimensional hybrid simulation code of *Winske and Omidi* [1993] to include a recycle algorithm which periodically changes velocities of superthermal superparticles. These simulations, which are generally similar to the "recycled" simulations of *Ambrosiano and Brecht* [1987] and *McKean et al.* [1992a] or the "refreshed" simulations of *Denton et al.* [1993], are described in detail in *Gary et al.* [1994a]. If our recycling algorithm does not strongly perturb the ions, ion anisotropy instabilities will continue to grow and the quasi-steady balance we seek will be established.

Figure 3 shows results from one such simulation. The growth of the fluctuating magnetic field energy density to saturation indicates that the instability is indeed flourishing here. The proton temperature anisotropy undergoes an initial phase in which the system develops its response to the recycling process, then enters a state in which it remains relatively constant with time. In contrast, the late-time response of $\beta_{\parallel p}$ shows a gradual diminuation; because n_p and $\mathbf{B}_o$ are constant in these simulations, the decrease in β reflects the result that the recycling procedure not only reduces $T_{\parallel p}$ but also removes ion kinetic energy from the system.

Figure 4 exhibits results from an ensemble of fifteen driven simulations. The solid circles represent the anisotropy values corresponding to the early-time maximum of the proton temperature anisotropy (See Figure 3), whereas the solid squares show late-time values of the anisotropy from the same runs. A detailed discussion of these results is given in *Gary et al.* [1994a]; the solid line of Figure 4 represents the least-squares fit of the late-time results:

$$\frac{T_{\perp p}}{T_{\parallel p}} - 1 = \frac{0.55}{\beta_{\parallel p}^{0.52}} \tag{4}$$

The similarity between the late-time results of the initial value and the recycled simulations is strong evidence that our recycle algorithm has not disturbed the wave-particle scattering process which drives the plasma toward instability threshold.

Denton et al. [1994b] have developed a bounded anisotropy model for describing the evolution of proton temperatures in the magnetosheath. Figure 5, which is taken from that paper, illustrate several relevant quantities observed from AMPTE/CCE as the spacecraft made a single crossing of the sheath. Here the quantities are plotted as a function of $\beta_{\parallel p}$ so that data from the magnetosheath proper appears toward the right and data from the plasma depletion layer toward the left. The approximate constancy of $p_{\perp tot}$ in the bottom panel of this figure indicates that conditions in the subsolar magnetosheath were approximately constant during this spacecraft transit.

Three curves are shown in the top three panels of Figure 5 for comparison against the data (crosses). The short dashed lines represent the predictions of adiabatic theory in which $T_{\perp p} = T_{\parallel p}$; this approach obviously predicts a $T_{\perp p}$ which is smaller than that observed and a $T_{\parallel p}$ which is larger than observations. In contrast, the long dashed lines illustrate the predictions of double adiabatic theory [*Chew et al.*, 1956] in which there is no coupling between the parallel and perpendicular proton temperatures. In this case the opposite result obtains; $T_{\perp p}$ is too large and $T_{\| p}$ is too small to match the observations. The solid lines in Figure 5 represent the results of the bounded anisotropy theory in which the proton anisotropy may not be larger than the observed value (See the top panel). This model yields quite good agreement with the observed evolution of both the perpendicular and parallel proton temperatures. The model even reproduces the temperature fluctuations observed as the spacecraft traversed the magnetosheath.

In summary, AMPTE/CCE observations have found a inverse correlation between the proton temperature anisotropy and $\beta_{\| p}$ in the highly compressed terrestrial magnetosheath [Equation (1)]. We have obtained similar correlations from the linear theory threshold condition of the proton cyclotron anisotropy instability [Equation (3)], from initial-value hybrid simulations of this instability, and from driven hybrid simulations of the same growing mode [Equation (4)]. The theory and simulations show that the observations may be interpreted as an upper bound for the proton anisotropy, imposed by the growth and wave-particle scattering of the proton cyclotron instability. The successful application of this bound to the prediction of $T_{\perp p}$ and $T_{\| p}$ observed during an AMPTE/CCE sheath crossing implies that this relationship represents a limited closure relation for the equations of anisotropic MHD that should provide more accurate descriptions of sheath flow as well as more accurate boundary conditions for magnetopause dynamics including reconnection. Although this closure relation is limited in the sense that it applies only if the protons have a bi-Maxwellian distribution with $T_{\perp p}$ sufficiently larger than $T_{\| p}$, it is quite general in the sense that it should be valid in any such plasma in which the field-aligned gradient scale lengths are long compared to an instability wavelength. Thus with minor modifications it should also be applicable to anisotropic MHD models of the terrestrial magnetosphere, Earth's magnetotail, and other planetary magnetosheaths.

Acknowledgments

The research described in this review was the result of collaborations among the following individuals: Brian J. Anderson of the Applied Physics Laboratory, Johns Hopkins University; Richard E. Denton of Dartmouth College; Stephen A. Fuselier of Lockheed Palo Alto Research Laboratory; Michael E. McKean formerly of Los Alamos National Laboratory and presently at the University of California, San Diego; Dan Winske of Los Alamos; and myself. I wish to acknowledge the substantial contributions of each of these people to the attainment of the results described here. My part of this work was performed under the auspices of the U.S. Department of Energy (DOE) and was supported by the DOE Office of Basic Energy Sciences, Division of Engineering and Geosciences, and the Space Plasma Theory Program of the National Aeronautics and Space Administration (NASA).

References

Ambrosiano, J., and S. H. Brecht, A simulation study of the Alfvén ion-cyclotron instability in high-beta plasmas, *Phys. Fluids*, **30**, 108, 1987.

Anderson, B. J., Magnetic ULF signals observed near the magnetopause, AGU Chapman Conference on the Magnetopause, San Diego, 14-18 March 1994.

Anderson, B. J., and S. A. Fuselier, Magnetic pulsations from 0.1 to 4.0 Hz and associated plasma properties in the Earth's subsolar magnetosheath and plasma depletion layer, *J. Geophys. Res.*, **98**, 1461, 1993.

Anderson, B. J., S. A. Fuselier, and D. Murr, Electromagnetic ion cyclotron waves observed in the plasma depletion layer, *Geophys. Res. Lett.*, **18**, 1955, 1991.

Anderson, B. J., S. A. Fuselier, S. P. Gary and R. E. Denton, Magnetic spectral signatures in the Earth's magnetosheath and plasma depletion layer, *J. Geophys. Res.*, **99**, 5877, 1994.

Chew, G. F., M. L. Goldberger, and F. E. Low, The Boltzmann equation and the one-fluid hydromagnetic equations in the absence of particle collisions, *Proc. Roy. Soc., Ser. A*, **236**, 112, 1956.

Denton, R. E., M. K. Hudson, S. A. Fuselier, and R. J. Anderson, Electromagnetic ion cyclotron waves in the magnetosheath plasma depletion layer, *J. Geophys. Res.*, **98**, 13,477, 1993.

Denton, R. E., S. P. Gary, B. J. Anderson, S. A. Fuselier, and M. K. Hudson, Low-frequency magnetic fluctuation spectra in the magnetosheath and plasma depletion layer, *J. Geophys. Res.*, **99**, 5893, 1994a.

Denton, R. E., B. J. Anderson, S. P. Gary, and S. A. Fuselier, Bounded anisotropy fluid model, *J. Geophys. Res.*, **99**, xxxxx, 1994b.

Fuselier, S. A., B. J. Anderson, S. P. Gary, and R. E. Denton, Ion anisotropy/beta correlations in the Earth's quasi-parallel magnetosheath, *J. Geophys. Res.*, submitted, 1994.

Gary, S. P., *Theory of Space Plasma Microinstabilities*, Cambridge University Press, Cambridge, 1993.

Gary, S. P., M. D. Montgomery, W. C. Feldman, and D. W. Forslund, Proton temperature anisotropy instabilities in the solar wind, *J. Geophys. Res.*, **81**, 1241, 1976.

Gary, S. P., S. A. Fuselier, and B. J. Anderson, Ion anisotropy instabilities in the magnetosheath, *J. Geophys. Res.*, **98**, 1481, 1993a.

Gary, S. P., B. J. Anderson, R. E. Denton, S. A. Fuselier, M. E. McKean, and D. Winske, Ion anisotropies in the magnetosheath, *Geophys. Res. Lett.*, **18**, 1767, 1993b.

Gary, S. P., M. E. McKean, D. Winske, B. J. Anderson, R. E. Denton, and S. A. Fuselier, The proton cyclotron instability and the anisotropy/β correlation, *J. Geophys. Res.*, **99**, 5903, 1994a.

Gary, S. P., P. D. Convery, R. E. Denton, S. A. Fuselier, and B. J. Anderson, Proton and helium cyclotron anisotropy instability thresholds in the magnetosheath, *J. Geophys. Res.*, **99**, 5915, 1994b.

Gary, S. P., B. J. Anderson, R. E. Denton, S. A. Fuselier, and M. E. McKean, A limited closure relation for anisotropic plasmas from the Earth's magnetosheath, *Phys. Plasmas*, **1**, xxxx, 1994c.

Kennel, C. F., and H. E. Petschek, Limit on stably trapped particle fluxes, *J. Geophys. Res.*, **71**, 1, 1966.

Manheimer, W., and J. P. Boris, Marginal stability analysis–A simpler approach to anomalous transport in plasmas, *Comments Plasma Phys. Cont. Fusion*, **3**, 15, 1977.

McKean, M. E., D. Winske, and S. P. Gary, Kinetic properties of mirror waves in magnetosheath plasmas, *Geophys. Res. Lett.*, **19**, 1331, 1992a.

McKean, M. E., D. Winske, and S. P. Gary, Mirror and ion cyclotron anisotropy instabilities in the magnetosheath, *J. Geophys. Res.*, **97**, 19,421, 1992b.

McKean, M. E., D. Winske, and S. P. Gary, Two-dimensional simulations of ion anisotropy instabilities in the magnetosheath, *J. Geophys. Res.*, **99**, xxxxx, 1994.

Phan, T.-D., G. Paschmann, W. Baumjohann, N. Sckopke, and H. Lühr, The magnetosheath region adjacent to the dayside magnetopause: AMPTE/IRM observations, *J. Geophys. Res.*, **99**, 121, 1994.

Sckopke, N., G. Paschmann, A. L. Brinca, C. W. Carlson, and H. Lühr, Ion thermalization in quasi-perpendicular shocks involving reflected ions, *J. Geophys. Res.*, **95**, 6337, 1990.

Song, P., C. T. Russell, and C. Y. Huang, Wave properties near the subsolar magnetopause: Pc 1 waves in the sheath transition layer, *J. Geophys. Res.*, **98**, 5907, 1993.

Tsurutani, B. T., E. J. Smith, R. R. Anderson, K. W. Ogilvie, J. D. Scudder, D. N. Baker, and S. J. Bame, Lion roars and nonoscillatory drift mirror waves in the magnetosheath, *J. Geophys. Res.*, **87**, 6060, 1982.

Winske, D., and N. Omidi, Hybrid codes: Methods and applications, in *Computer*

Space Plasma Physics: Simulation Techniques and Software, Edited by H. Matsumoto and Y. Omura,p. 103, Terra Scientific Publishers, Tokyo, 1993.

Figure Captions

Figure 1. Proton temperature anisotropies at the thresholds of the proton cyclotron and mirror instabilities as a function of $\beta_{\parallel p}$. The solid symbols represent numerical solutions of the linear Vlasov dispersion equation [*Gary*, 1993] at $\gamma_m = 0.01\Omega_p$ for the proton cyclotron instability (circles) and for the mirror instability (triangles). The lines represent analytic expressions fitting these results: the dashed line is Equation (2) and the solid line is Equation (3). Anisotropies greater than threshold correspond to faster instability growth; anisotropies less than threshold imply slower growth or stability. The model here is that of an electron-proton plasma with $T_e = 0.25T_p$ (After *Gary et al.*, 1994c).

Figure 2. Proton temperature anisotropy as a function of $\beta_{\parallel p}$; results from the asymptotic states of initial-value hybrid computer simulations using the magnetosheath parameter model of *Gary et al.* [1993b]. Here the solid squares represent results from one-dimensional simulations of ion cyclotron anisotropy instabilities, the $\times$ symbols show results from one-dimensional simulations of the mirror instability, and the open squares represent results from two-dimensional simulations in which both instability types may arise. The solid line represents an approximate fit to the AMPTE/CCE observations (From *Gary et al.*, 1993b).

Figure 3. Results from a driven simulation of the proton cyclotron anisotropy instability in an electron/proton plasma. The initial parameters here are $\beta_{\parallel p} = 1.00$ and $T_{\perp p}/T_{\parallel p} = 1.58$. The three panels here represent the total fluctuating magnetic field energy, the proton temperature anisotropy, and the proton parallel β (From *Gary et al.*, 1994a).

Figure 4. The proton anisotropy from an ensemble of driven simulations of the proton cyclotron anisotropy instability in an electron/proton plasma as a function of $\beta_{\parallel p}$. For this ensemble of runs, the initial values of $\beta_{\parallel p}$ ranged from 0.25 to 10.0. The solid circles represent the maximum early-time value of the anisotropy from each simulation; the solid squares show corresponding late-time anisotropies. The line represents the least-squares fit to the late-time results, Equation (4) (From *Gary et al.*, 1994a).

Figure 5. The proton temperature anisotropy, the perpendicular proton temperature (in keV), the parallel proton temperature (in keV), and the total (plasma plus magnetic) perpendicular pressure (in units of 10^{-6} dyne/cm^2) as functions of $\beta_{\parallel p}$. The curves represent predictions of three theories: isotropic adiabatic theory (small dashes), double

adiabatic theory (large dashes), and the bounded anisotropy model (solid lines). Observations from CCE are plotted as plus signs (From *Denton et al.*, 1994b).

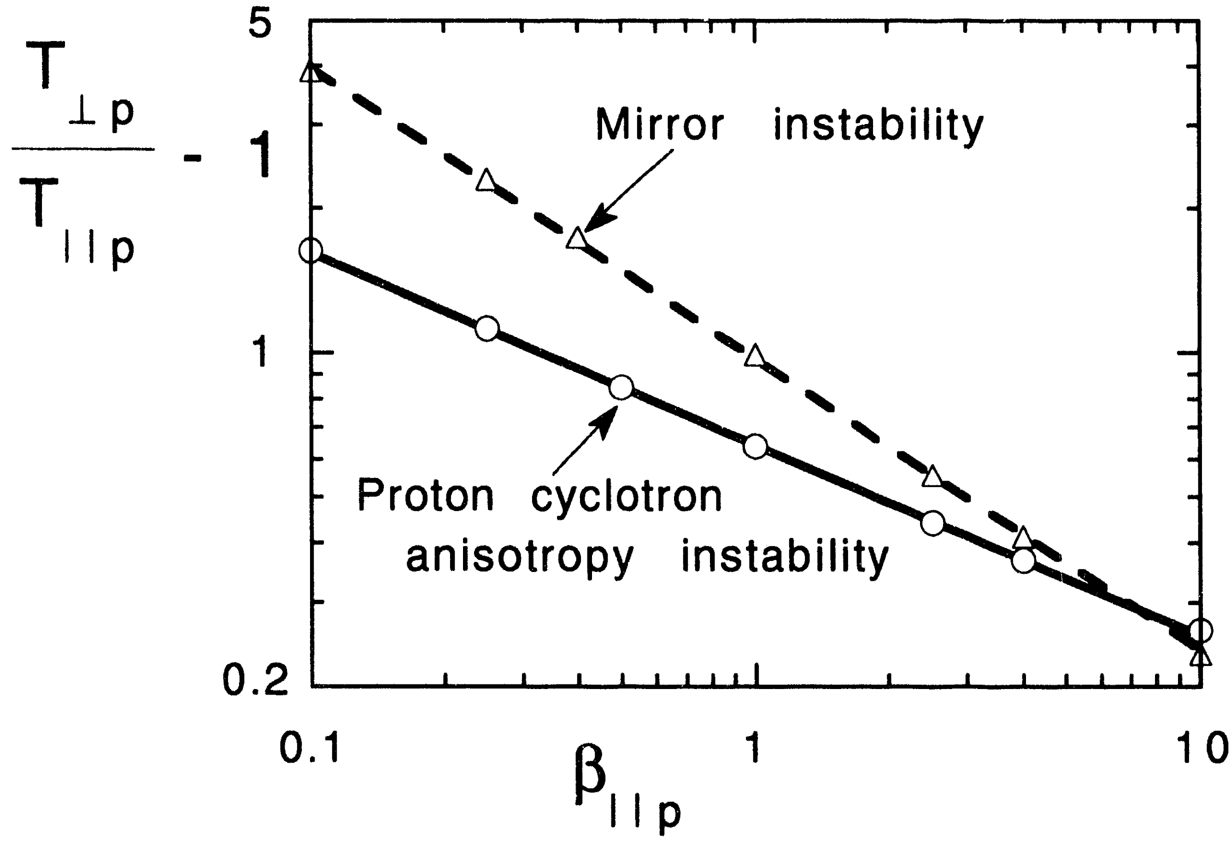
$\frac{T_{\perp p}}{T_{\parallel p}} - 1$
5
1
0.2
0.1
1
10
$\beta_{\parallel p}$
Mirror instability
Proton cyclotron
anisotropy instability

Figure 1

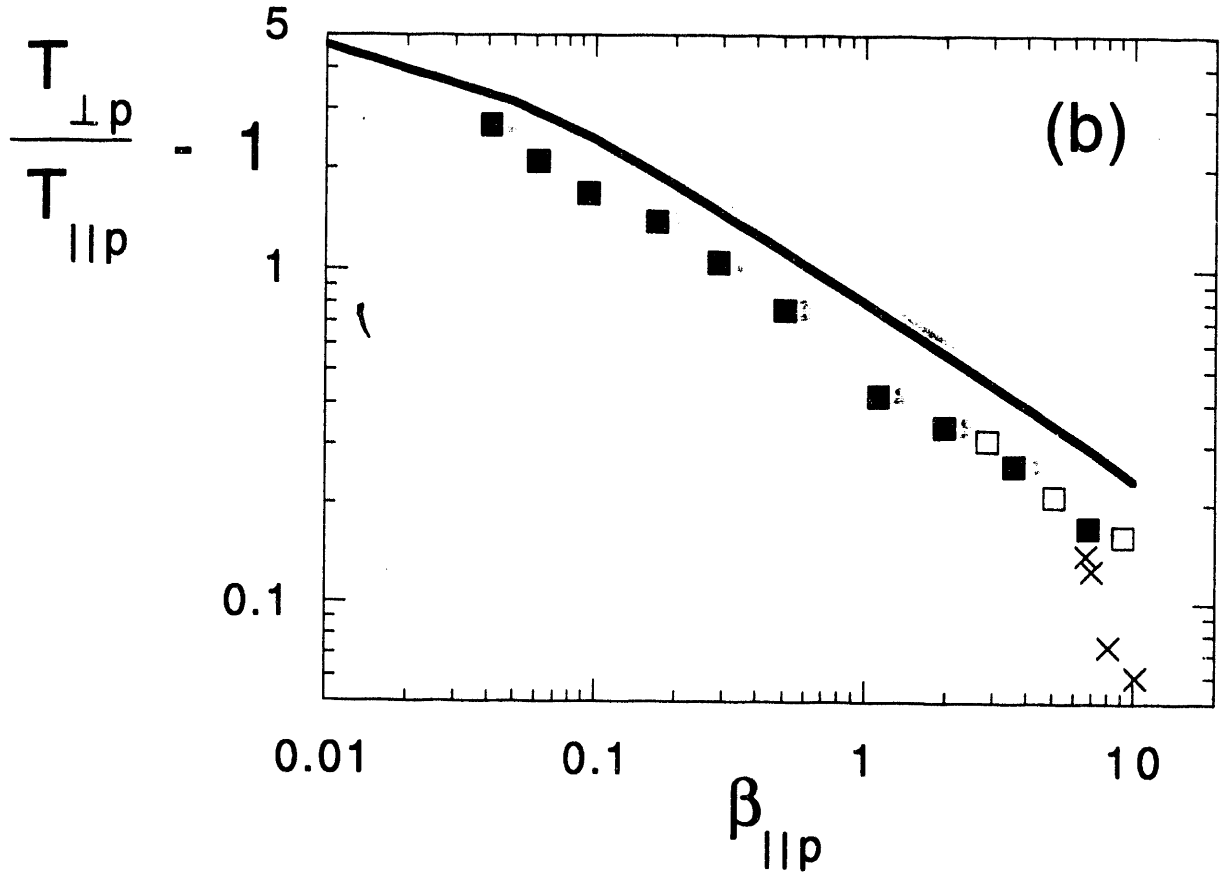

Figure 2

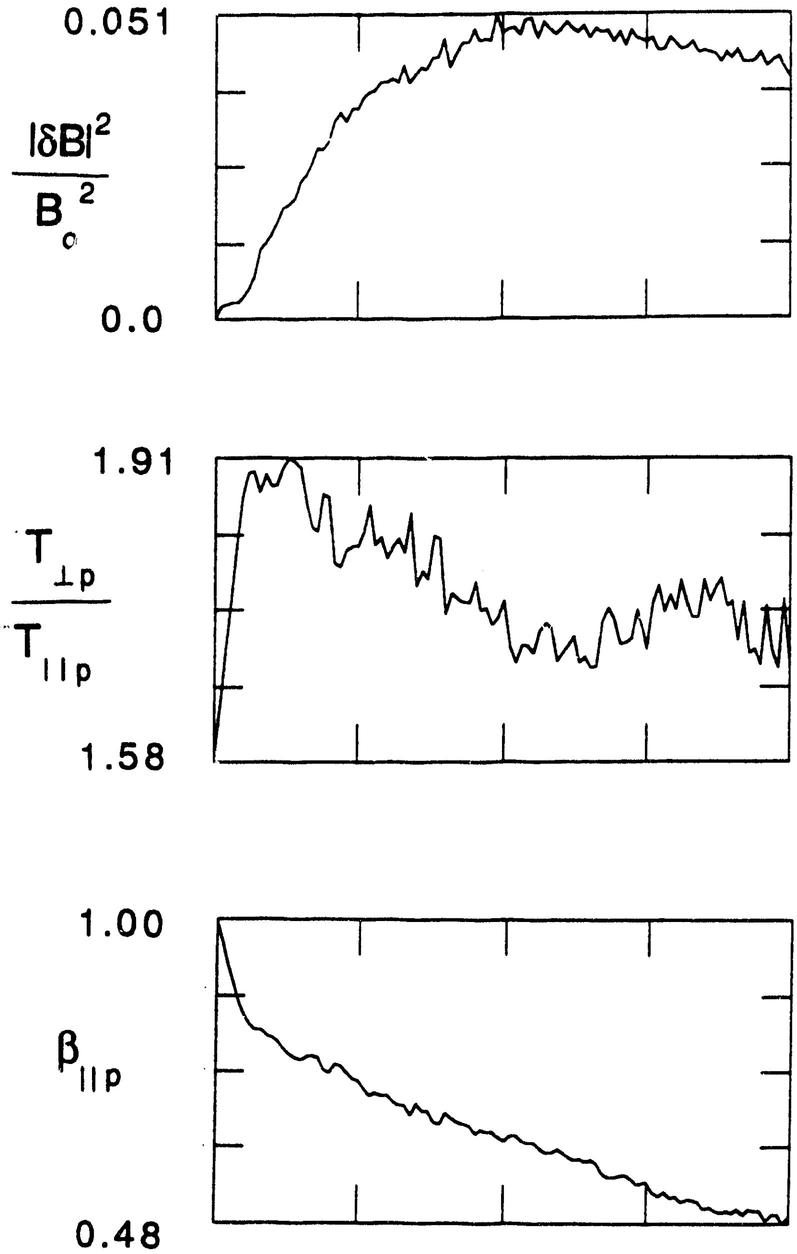
0.051
$|\delta B|^2 / B_o^2$
0.0
1.91
$T_{\perp p} / T_{\parallel p}$
1.58
1.00
$\beta_{\parallel p}$
0.48

Figure 3

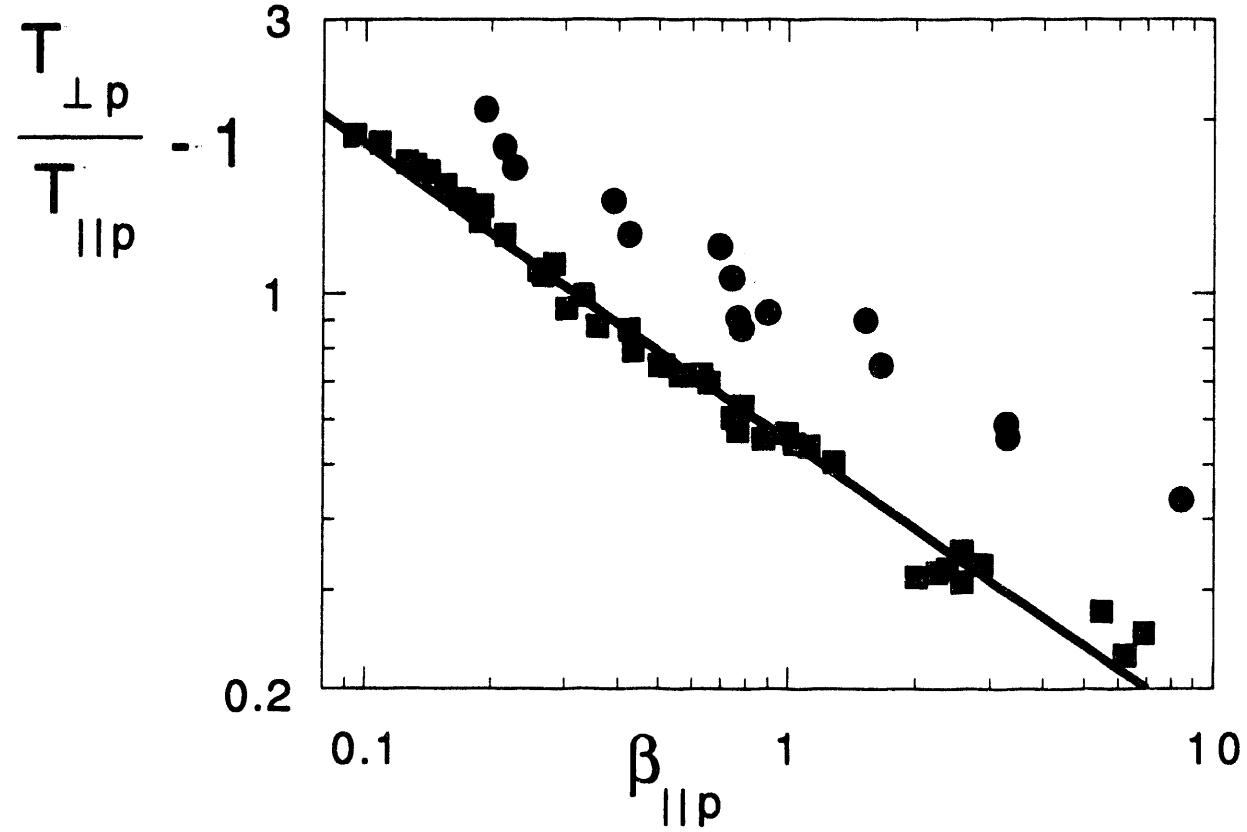

Figure 4

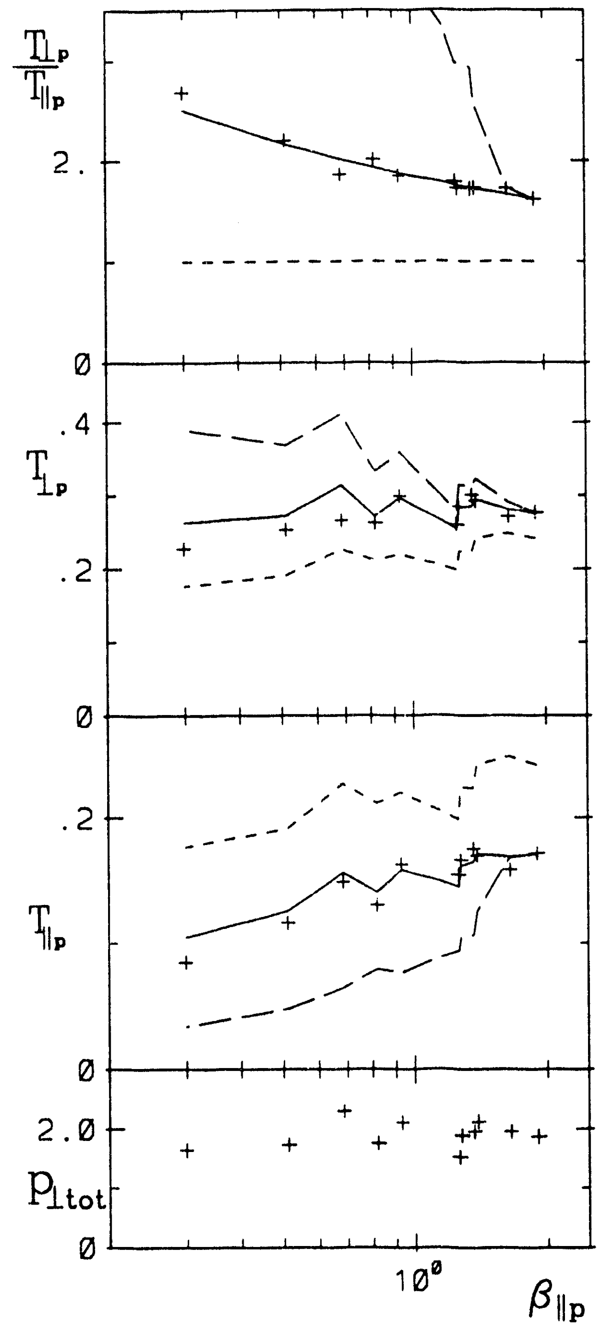

$\frac{T_{\perp p}}{T_{\parallel p}}$
2.
0
.4
$T_{\perp p}$
.2
0
.2
$T_{\parallel p}$
0
2.0
$p_{\perp tot}$
0
10^0
$\beta_{\parallel p}$

Figure 5

DATE
FILMED
10/19/94

END